

Lawrence Berkeley National Laboratory

Recent Work

Title

DESIGN OF PERMANENT MULTIPOLE MAGNETS WITH ORIENTED RARE EARTH COBALT MATERIAL

Permalink

<https://escholarship.org/uc/item/20b829tr>

Author

Halbach, K.

Publication Date

1979-08-01



Lawrence Berkeley Laboratory

UNIVERSITY OF CALIFORNIA, BERKELEY

Engineering & Technical Services Division

Submitted to Nuclear Instruments and Methods

DESIGN OF PERMANENT MULTIPOLE MAGNETS WITH ORIENTED RARE EARTH COBALT MATERIAL

K. Halbach

August 1979

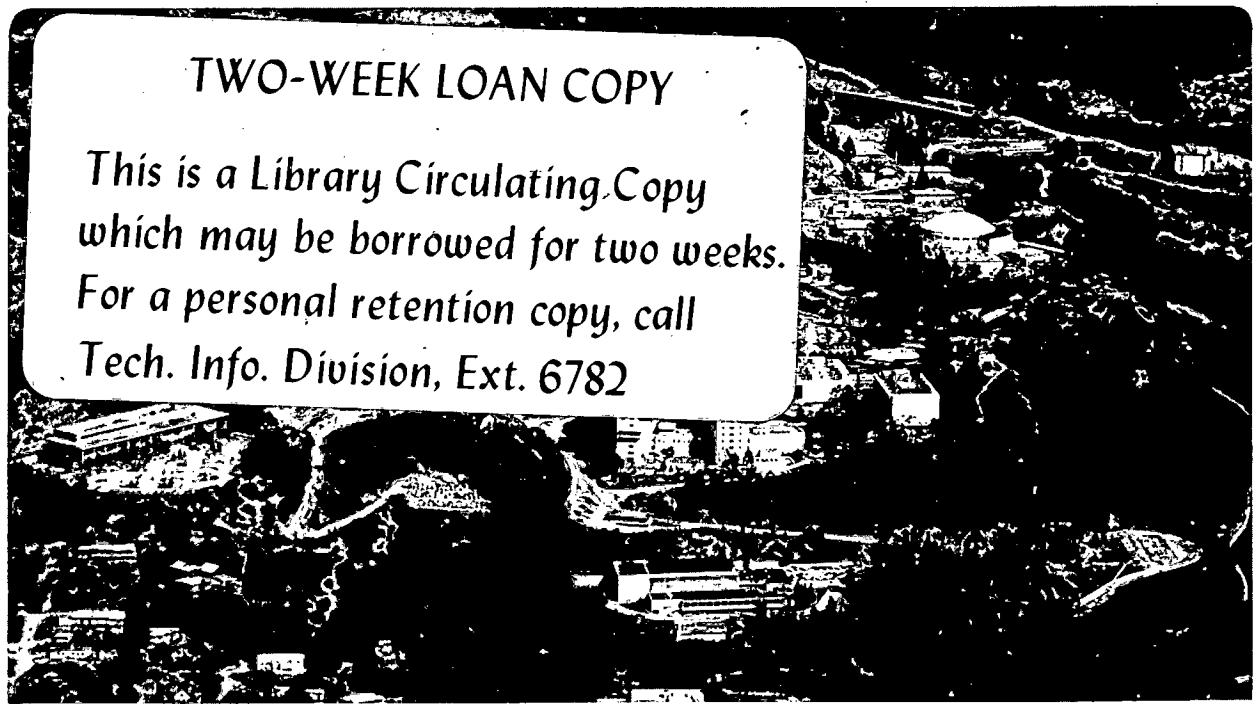
RECEIVED
LAWRENCE
BERKELEY LABORATORY

SEP 14 1979

LIBRARY AND
DOCUMENTS SECTION

TWO-WEEK LOAN COPY

This is a Library Circulating Copy which may be borrowed for two weeks. For a personal retention copy, call Tech. Info. Division, Ext. 6782



Prepared for the U. S. Department of Energy
under Contract W-7405-ENG-48

LBL-9604/c.2

DISCLAIMER

This document was prepared as an account of work sponsored by the United States Government. While this document is believed to contain correct information, neither the United States Government nor any agency thereof, nor the Regents of the University of California, nor any of their employees, makes any warranty, express or implied, or assumes any legal responsibility for the accuracy, completeness, or usefulness of any information, apparatus, product, or process disclosed, or represents that its use would not infringe privately owned rights. Reference herein to any specific commercial product, process, or service by its trade name, trademark, manufacturer, or otherwise, does not necessarily constitute or imply its endorsement, recommendation, or favoring by the United States Government or any agency thereof, or the Regents of the University of California. The views and opinions of authors expressed herein do not necessarily state or reflect those of the United States Government or any agency thereof or the Regents of the University of California.

DESIGN OF PERMANENT MULTIPOLE MAGNETS WITH ORIENTED RARE EARTH COBALT MATERIAL

K. Halbach
University of California
Lawrence Berkeley Laboratory
Berkeley, CA 94720

Abstract

By taking advantage of both the magnetic strength and the astounding simplicity of the magnetic properties of oriented Rare Earth Cobalt material, new designs have been developed for a number of devices. In this article on multipole magnets, special emphasis is put on quadrupoles because of their frequent use and because the achievable aperture fields (1.2-1.4T) are rather large. This paper also lays the foundation for future papers on a) linear arrays for use as "plasma buckets" or undulators for the production of synchrotron radiation; b) structures for the production of solenoidal fields, and c) three-dimensional structures such as helical undulators or multipoles.

1) Introduction

For some applications, the most important of the many advantages of permanent magnets is the fact that they can be made very small without reduction of magnetic field strength. In conventionally powered magnets, the current density in the coils is inversely - proportional to the linear dimension, leading to insurmountable cooling problems and attendant reduction of field strength as size decreases.

We will discuss new designs that, with currently available oriented Rare Earth Cobalt (REC) material, produce, in some devices, fields that are as strong or stronger than those achievable with conventional magnets of any size.

Thus, REC magnets will have a performance advantage over conventional magnets regardless of size, shifting the decision between the two to different areas, such as convenience of strength adjustment, price, etc.

The advantage of REC is not only its strength, but also the simplicity of its magnetic properties. This simplicity makes REC systems easy to understand and to treat analytically, which in turn leads directly to improved designs. For this reason, we devote some space to REC properties, and how they can be best described in the magnetostatic equations, despite the fact that these properties have been known by workers in the field since Strnat¹⁾ started the development of REC.

For the sake of completeness, we include similarly the derivation of some theorems that are, at least in principle, textbook material, but are used so infrequently that they cannot be expected to be at the fingertips of most readers.

2) Basic formulae, notation

For three dimensional (3D) calculations, we use the standard Cartesian coordinates x, y, z . Most of the two dimensional (2D) calculations are done with complex numbers that are identified by underlining the symbol. Specifically \underline{z} is defined by $\underline{z} = x + iy = r e^{i\varphi}$, with $i^2 = -1$. The complex conjugate of a quantity is indicated by an asterisk.

In a vacuum region, the two dimensional field components B_x, B_y (or H_x, H_y) can be derived from either a scalar potential V or a vector potential that needs to have only a component A in the z direction:

$$B_x = \partial A / \partial y = -\partial V / \partial x \quad (1a)$$

$$B_y = -\partial A / \partial x = -\partial V / \partial y. \quad (1b)$$

The relationships between the derivatives of A and V are the same as the Cauchy-Riemann conditions of the real and imaginary part of an analytical function of the complex variable \underline{z} , i.e., the complex potential $\underline{F}(\underline{z}) = A + iV$ is such a function, and if we use $\underline{B} = B_x + i B_y$ to describe the two-dimensional vector \vec{B} , it follows from equ. 1 that

$$\underline{B}^* = i \underline{dF/dz} \quad (2)$$

is also an analytical function of \underline{z} . The field at location \underline{z}_0 , generated by a current filament, I, at location \underline{z} , is given by

$$\underline{B}^*(\underline{z}_0) = \frac{\mu_0 I}{2\pi i} \cdot \frac{1}{\underline{z}_0 - \underline{z}} \quad (3)$$

The coefficients of the Taylor series expansion of \underline{F} and \underline{B}^* are in the customary fashion identified by the subscript of the expansion of \underline{F} :

$$\underline{F}(\underline{z}_0) = \sum_{n=1}^{\infty} \underline{a}_n \underline{z}_0^n \quad (4a)$$

$$\underline{B}^*(\underline{z}_0) = \sum_{n=1}^{\infty} \underline{b}_n \underline{z}_0^{n-1}; \quad \underline{b}_n = i n \underline{a}_n. \quad (4b)$$

The same expansions, but with $n < 0$, will be used to describe fields in the region radially outside of magnets. MKS units are used throughout, with

$$\mu_0 = 4\pi \cdot 10^{-7} \text{ Vsec } \bar{A}^{-1} \bar{m}^{-1}.$$

3) Properties of REC

3.1) The manufacturing process.

To get a rough understanding of the reasons for the REC properties described in sect. 3.2, we describe very briefly the major steps in one of the major manufacturing processes used today to produce REC. For details, the reader is referred to the book by McCaig².

After a molten mixture of roughly five (atomic) parts Cobalt to one (atomic) part of some Rare Earth metal(s) is solidified by rapid cooling, a crushing and milling process produces a powder that consists of particles with linear dimensions of the order of $5\mu\text{m}$. These grains are magnetically highly anisotropic, "wanting" to be polarized only along one crystalline direction. The powder is then exposed to a strong magnetic field and subjected to high pressure, causing the individual grains to physically rotate until their magnetically preferred axes are parallel to the applied field. These aligned blocks of material are then sintered, and machined or ground if necessary. Finally the material is exposed to a very strong magnetic field in a direction parallel or antiparallel to the previously established preferred direction, orienting practically all alignable magnetic moments along the direction of magnetization, commonly called the easy axis. The property that makes REC so valuable is that this magnetization is very strong, and that it can be changed in a substantial way only by applying a strong field in the direction opposite to the one used to magnetize the material.

3.2) The $\vec{B}(\vec{H})$ relationship of REC.

The relationship between $B_{||}$ and $H_{||}$ in the direction parallel to the easy axis is schematically shown in Fig. 1. The most important characteristics of the $B_{||}(H_{||})$ curve are the following:

- a) It is, for all intents and purposes, a straight line over a very wide range, with a typical slope $dB_{||} / dH_{||} \mu_0 = \mu_{||} \approx 1.04-1.08$. The point where the slope becomes significantly larger depends on the details of the manufacturing process, but is usually well within the third quadrant, at $-H_{||} / H_c \approx 1.5-2$.
- b) The offset of the $B_{||} (H_{||})$ curve from the origin, the remanent field B_r , is typically .8T to .95T, which is the coercive field $\mu_0 H_c$ about 4-8% less than B_r .
- c) As long as one stays on the straight line part of the $B_{||} (H_{||})$ curve, moving along the curve does not change this straight line.

In the range of interest here, the relationship between $B_{||}$ and $H_{||}$ can be represented by:

$$B_{||} = \mu_0 \mu_{||} H_{||} + B_r \quad (5a)$$

or, with $\gamma = 1/\mu$:

$$H_{||} = \gamma_{||} B_{||} / \mu_0 - H_c \quad (5b)$$

In the direction perpendicular to the easy axis, the relationship between B_{\perp} and H_{\perp} is, to very good approximation, described by:

$$B_{\perp} = \mu_0 H_{\perp} + B_r \cdot \frac{H_{\perp}}{H_A}$$

or, with

$$\mu_{\perp} = 1/\gamma_{\perp} = 1 + B_r/\mu_0 H_A,$$

$$B_{\perp} = \mu_0 \mu_{\perp} H_{\perp} \quad (6)$$

The high degree of anisotropy of good material manifests itself in the large values of the anisotropy field $\mu_0 H_A$: typical values are 12-40T, giving values of 1.02 to 1.08 for μ_{\perp} , and equ. (6) is usually valid up to several Tesla.

Aside from the REC material discussed so far, resin bonded REC material is also available, with qualitatively the same properties, but lower values of B_r and H_c . Some of the oriented ferrites have also similar properties, but with $B_r \leq .35T$ and larger values (≈ 1.1) for the permeabilities μ_{\parallel} and μ_{\perp} .

The designs discussed in this paper can also be implemented with these materials; we always refer to REC magnets because it is the unique strength of the REC materials, combined with the other properties described in this section, that will open the door to new and exciting applications.

3.3) Description of REC properties in the magnetostatic equations.

Equ's. (5a) and (6) can be combined into the vector equation:

$$\vec{B} = \mu_0 \vec{\mu}^* \vec{H} + \vec{B}_r. \quad (7a)$$

In this equation, \vec{B}_r is the vector with the magnitude of the remanent field B_r in the direction of the easy axis, and $\vec{\mu}^* \vec{H} = \mu_{\perp} \vec{H}_{\perp} + \mu_{\parallel} \vec{H}_{\parallel}$. Equ's. (5b) and (6) can be similarly combined into

$$\vec{H} = \vec{J}^* \vec{B} / \mu_0 - \vec{H}_c. \quad (7b)$$

If we derive \vec{H} from a scalar potential, we have to satisfy $\text{div } \vec{B} = 0$, yielding with equ. (7a)

$$\text{div } (\mu_0 \vec{\mu}^* \vec{H}) = \mathcal{S} = - \text{div } \vec{B}_r. \quad (8a)$$

If we derive similarly \vec{B} from a vector potential, we get from equ. (7b) and Ampères law

$$\text{curl } \vec{y} * \vec{B}/\mu_0 = \vec{j} = \text{curl } \vec{H}_C. \quad (8b)$$

The anisotropy of the material shows up in two different ways: in the inhomogeneous terms on the right sides of equ's. (8), and in the slight anisotropy associated with the weak differential permeability of REC. Because the permeabilities are so close to one, we assume, unless stated otherwise, that $\mu_{||} = \mu_{\perp} = 1$. This very good approximation, together with the assumption of constant H_C and B_r , means that the material can be treated as vacuum with either an imprinted charge density $-\text{div } \vec{B}_r$ or an imprinted current density $\text{curl } \vec{H}_C$. This in turn has the consequence that the fields produced by different pieces of REC superimpose linearly, and that they can be calculated with fairly little effort when no soft magnetic material is present. It should be noted that in case of homogeneously magnetized material, i.e., $\vec{H}_C, \vec{B}_r = \text{const.}$ within the material, $\text{curl } \vec{H}_C$ and $\text{div } \vec{B}_r$ are zero everywhere except at the surface, where one encounters delta functions that signify the presence of current sheets or charge sheets.

3.4) Calculation of three dimensional (3D) fields produced by REC.

In the absence of soft material, we derive the field at the location outside the material from a scalar potential,

$$\vec{H}(\vec{r}_0) = - \text{grad } V, \quad (9)$$

with V given by an integral over the volume of the material:

$$\mu_0 V(\vec{r}_0) = \frac{1}{4\pi} \int \frac{\rho(\vec{r})}{|\vec{r} - \vec{r}_0|} dv. \quad (10)$$

a

In case of homogeneously magnetized REC piece, one has a charge sheet at its surface. With equ. (8a) one therefore obtains in that case V from an integral over the surface of the material:

$$V = \frac{1}{4\pi} \int \frac{\vec{H}_c \cdot d\vec{a}}{|\vec{r} - \vec{r}_0|} = \frac{\vec{H}_c}{4\pi} \cdot \int \frac{d\vec{a}}{|\vec{r} - \vec{r}_0|} \quad (11)$$

It has been used that, for our model, $\vec{B}_r = \mu_0 \vec{H}_c$. A particularly appealing property of this formula is the fact that the integral is independent of \vec{H}_c .

For the case of continuously varying \vec{H}_c , we use, with $K(\vec{r}) = \frac{1}{|\vec{r} - \vec{r}_0|}$ the identity

$$\nabla K / \mu_0 = -K \operatorname{div} \vec{H}_c = \vec{H}_c \operatorname{grad} K - \operatorname{div} (K \vec{H}_c).$$

Because $\vec{H}_c = 0$ outside the material, $\int \operatorname{div} (K \vec{H}_c) dv = \int K \vec{H}_c \cdot d\vec{a} = 0$.

With $\operatorname{grad} K = -\frac{\vec{r} - \vec{r}_0}{|\vec{r} - \vec{r}_0|^3}$, we obtain

$$V = -\frac{1}{4\pi} \int \frac{\vec{H}_c \cdot (\vec{r} - \vec{r}_0)}{|\vec{r} - \vec{r}_0|^3} dv \quad (12)$$

3.4) Calculation of two-dimension (2D) fields produced by REC.

For a REC assembly that is sufficiently long in the z-direction and whose magnetization vector \vec{B}_r has no z component, the fields outside the material can in the absence of soft steel in good approximation be described by:

$$\underline{B}^*(z_0) = \frac{\mu_0}{2\pi i} \int \frac{1}{\underline{z}_0 - \underline{z}} dx dy, \quad (13)$$

with

$$\mu_0 j = \partial B_{ry} / \partial x - \partial B_{rx} / \partial y. \quad (14)$$

We have again used $B_r = \mu_0 H_c$.

It is shown in the Appendix that equ. (13) can, without restrictions on $\underline{B}_r = B_{rx} + i B_{ry}$, be written as

$$\underline{B}^*(z_0) = \frac{1}{2\pi} \int \frac{B_r}{(z_0 - z)^2} dx dy. \quad (15)$$

This formula can be considered the 2D equivalent of equ. (12), because it expresses the field by an integral that contains the magnetization itself, and not a combination of its spatial derivatives.

Equ. (15) has a property that is highly significant for many applications: If two REC assemblies are identical, except that in the second system the easy axis is rotated everywhere by the angle $+\beta$ relative to the easy axis orientation in first system, then the right hand side of equ. (15) for the second system equals that of the first system, but is multiplied by $e^{i\beta}$. This allows us to state the

Easy Axis Rotation Theorem: If in a 2D, soft steel free, REC system all easy axes are rotated by the angle $+\beta$, then all magnetic fields outside the REC rotate by the angle $-\beta$ without a change in amplitude.

Fig. 2 illustrates this theorem. The theorem is qualitatively easy to understand if one realizes that each volume element of REC produces a dipole field for which this theorem is valid for obvious reasons.

For a homogeneously magnetized piece of REC, \underline{B}_r can be taken outside the integral in equ. (15). Integrating first over x, one obtains:

$$\underline{B}^*(z_0) = \frac{B_r}{2\pi} \oint \frac{dy}{z_0 - z}. \quad (16a)$$

Integration over y first yields

$$\underline{B}^*(z_0) = - \frac{B_r}{2\pi i} \oint \frac{dx}{z_0 - z} \quad (16b)$$

and equ's. (16a) and (16b) can be combined into

$$\underline{B}^*(z_0) = - \frac{B_r}{4\pi i} \oint \frac{dz^*}{z_0 - z} \quad (16c)$$

The last three equations are given because, depending on the geometrical shape of the REC piece, one of these integrals may be easier to evaluate than the others or the integral in equ. (15).

Equ. (16b) (and similarly equ. (16a)) can also be derived by using the current sheet model for a REC piece with its easy axis parallel to the x -axis, and then invoking the easy axis rotation theorem.

To calculate fields inside the material, the techniques developed in ref. 3 can be used. We summarize here only the result for the case of a homogeneously magnetized piece of REC: By first removing a circular cylinder of material around the point z_0 , any one of the equ's (16) can be used, with an integration path as shown in Fig. 3. (Notice that the integrals over the straight lines cancel.). To obtain \underline{B}^* , one has to add the contribution $B_r/2$ caused by the removed cylinder. To obtain $\mu_0 \underline{H}^*$ inside the material, one has to use $\mu_0 \underline{H}^* = \underline{B}^* - \underline{B}_r$.

Even though it is possible to write down explicitly the fields produced by the multipole magnets discussed below, it is more convenient, and gives more insight, to use the Taylor expansions introduced in equ's. (4). To obtain the expansion coefficients, one has to use in equ's. (16)

$$\frac{1}{z_0 - z} = - \sum_{n=1}^{\infty} \frac{z_0^{n-1}}{z^n} \quad (17a)$$

and for use in equ. (15), one obtains by differentiation of equ. (17a):

$$\frac{1}{(z_0 - z)^2} = \sum_{n=1}^{\infty} \frac{n z_0^{n-1}}{z^{n+1}} \quad (18a)$$

For a field expansion radially outside the magnet, one has to use

$$\frac{1}{z_0 - z} = \sum_{n=-1}^{-\infty} \frac{z_0^{n-1}}{z^n} \quad (17b)$$

and

$$\frac{1}{(z_0 - z)^2} = - \sum_{n=-1}^{-\infty} \frac{n \cdot z_0^{n-1}}{z^{n+1}} \quad (18b)$$

4) REC multipole magnets

4.1) Multipoles with continuous easy axis orientation.

To produce a strong $2N$ - multipole magnet with good field quality, one wants to arrange the REC in such a way that in equ. (4b), \underline{b}_N is large, and that all other \underline{b}_n are as small as possible. Using equ. (18a) in equ. (15), we obtain

$$\underline{b}_n = \frac{n}{2\pi} \int \frac{B_r}{z^{n+1}} da ,$$

With $\underline{B}_r = B_r e^{i\beta(\varphi)}$, and $\underline{z} = r e^{i\varphi}$, we get

$$\underline{b}_n = \frac{n}{2\pi} \int \frac{B_r \exp(i(\beta(\varphi) - (n+1)\varphi))}{r^{n+1}} r dr d\varphi \quad (19)$$

From this equation follows directly that the largest possible real \underline{b}_n is obtained by choosing

$$\beta(\varphi) = \varphi \cdot (N+1). \quad (20)$$

Equ. (19) also shows the expected fact that a piece of REC contributes the more to the multipole strength the closer it is to the point $\underline{z} = 0$.

If the space between the two circles $|\underline{z}| = r_1$ and $|\underline{z}| = r_2$ is filled with REC, with $B_r = \text{constant}$ and $\beta(\varphi)$ given by equ. (20), $\underline{b}_n = 0$ for $n \neq N$, giving for $|\underline{z}_0| < r_1$

$$\underline{B}^*(\underline{z}_0) = \left(\frac{\underline{z}_0}{r_1}\right)^{N-1} \cdot B_r \cdot \frac{N}{N-1} \cdot \left(1 - \left(\frac{r_1}{r_2}\right)^{N-1}\right) \quad \text{for } N \geq 2; \quad (21a)$$

$$\underline{B}^*(\underline{z}_0) = B_r \ln(r_2/r_1) \quad \text{for } N = 1. \quad (21b)$$

Inspection of the field for $|\underline{z}| > r_2$, using equ. (18b) instead of equ. (18a), shows that the field outside this multipole magnet is exactly zero.

The fact that "recipe" equ. (20) leads to a perfect multipole is not surprising when one realizes that as a direct consequence of equ. (20), the current density j (in equ. (8b)) inside the material has only the component $j_c = H_c \cdot (N+1) \cdot \sin N\varphi / r$, with the current sheets at the inside and outside boundaries of the REC being proportional to $\sin N\varphi$ also.

Equ's. (21) were given for $N=1,2$ by J.P. Blewett⁽⁴⁾ in an unpublished report in 1965. However that report does not mention the anisotropy of the material, and consequently does not give the design recipe represented by equ. (20).

The just discussed multipole obviously produces the strongest and cleanest multipole field possible within a circular aperture of a pure REC multipole with a given amount of material. A study of the field inside the material shows that one can find closed curves that are perpendicular to \vec{H} everywhere. Replacing the material inside such a closed curve by soft steel with very large permeability will reduce the amount of REC without changing the field in the aperture significantly. It is my subjective judgement that the potential savings are too small to be worth the resulting complication of construction in case of strong multipoles, and this avenue has therefore not been pursued in the study of the segmented multipoles.

Since the above mentioned steel contours can range into the aperture region, this approach can be used to design multipoles that have steel poles controlling the field in the aperture and use fairly little REC. However, with the exception of dipoles, those magnets have weaker pole tip fields than the pure REC multipoles. While it is my opinion that incorporation of steel into the design will not increase the upper limit of the achievable multipole strength, given by equ. (21a), I have no proof for this assessment.

In order to satisfy equ. (20), one needs during the alignment process strong magnetic fields with a distribution of local direction given by equ. (20). Since a 2D vacuum field satisfying that condition must behave like $B \sim 1/z^{N+1}$ in the region of interest, it is highly unlikely that one can produce REC with precisely the desired easy axis distribution,

particularly for small magnets. Fortunately, the segmented magnet design discussed below has a performance very close to that of the ideal REC multipole.

4.2) The segmented multipole magnet.

To get a reasonable approximation to equ. (20), we segment the magnet into M geometrically identical pieces such that, ignoring the direction of the easy axes, the structure is invariant to rotation by the angle $2\pi/M$ about $z=0$. Throughout each piece, the easy axis points in the same direction, but that direction advances (in the x-y coordinate system) by $(N+1) \cdot 2\pi/M$ from one piece to the next. This means that relative to a coordinate system fixed in the piece, the easy axis advances by $N \cdot 2\pi/M$ from one piece to the next.

Using equ's. (17), (16c) and (4b), \underline{b}_n produced by one such piece can be expressed (for both positive and negative n) by

$$\underline{b}_n = \text{sgn}(n) \frac{B_r}{4\pi i} \oint \frac{dz^*}{z^n} \quad (22)$$

If the contribution to \underline{b}_n coming from a reference piece is \underline{c}_n , then the contribution from a piece rotated by α relative to the reference piece is $\underline{c}_n \cdot e^{i\alpha(N+1)} \cdot e^{-i\alpha(n+1)}$, where the first exponential factor comes from the rotation of the easy axis by $\alpha(N+1)$, and the second factor from the integral in equ. (22). With $\alpha = m \cdot 2\pi/M$, we get for the whole assembly

$$\underline{b}_n = \underline{c}_n \cdot \sum_{m=0}^{N-1} e^{i2\pi m(N-n)/M}$$

If $(N-n)/M$ is zero or a positive or negative integer, the sum equals M. If $(N-n)/M$ is not an integer, the geometrical series is zero, yielding

$$\underline{b}_n^* (z_0) = M \sum_V \underline{c}_n z_0^{n-1}; \quad n = N + VM. \quad (23)$$

Depending whether one wants to know the fields in the aperture region or outside the magnet, one takes the sum over either positive or negative n .

Fig. 4 shows the geometry for a trapezoidal reference piece that is bisected by the x -axis and whose magnetization is characterized by B_r .

We allow discussion of a smaller than maximum possible angular size ($2\pi/M$) by making the angular size of the reference piece $\epsilon \cdot 2\pi/M$.

For $n > 0$, C_n is most easily obtained by using equ. (17a) in equ. (16b).

Using that C_n in equ. (23) gives:

$$B^*(z_0) = B_r \sum_{v=0}^{\infty} \left(\frac{z_0}{r_1} \right)^{n-1} \cdot \frac{n}{n-1} \cdot \left(1 - \left(\frac{r_1}{r_2} \right)^{n-1} \right) \cdot K_n$$

$$n = N + \gamma M$$

$$K_n = \cos^n(\epsilon \pi / M) \cdot \frac{\sin(n \epsilon \pi / M)}{n \pi / M}$$

$$\left[\frac{n}{n-1} \cdot \left(1 - \left(\frac{r_1}{r_2} \right)^{n-1} \right) \right]_{n=1} = \ln(r_2/r_1)$$
(24a)

For the geometry indicated by dashed lines in Fig. 4, i.e., for circular arcs of radii r_1 , r_2 as inner and outer boundaries, C_n is most easily calculated with equ's. (15) and (18a), and K_n in equ's. (24a) has to be replaced by

$$K_n = \frac{\sin((n+1) \cdot \epsilon \pi / M)}{(n+1) \pi / M}$$
(24b)

It follows from equ. (24) that for a given B_r , and for $n = N > 1$, there always exists an upper limit for the field strength at the magnet aperture, while for the dipole this upper limit is controlled in essence by the $B_{||}$ ($H_{||}$) curve in the third quadrant.

Comparison of equ's. (24) with equ's. (21) shows that the fundamental harmonic of the segmented multipole is smaller by a factor K_N than the equivalent ideal REC multipole and that for $\xi = 1$ one comes close to the ideal strength if the number of REC pieces per period,

$$M' = M/N, \quad (25)$$

is equal or larger than eight.

In the somewhat unusual case that one elects to use for M' a small value like 2, it follows in general from equ's. (15) and (18a) (and specifically, of course, from equ's. 24) that K_N is largest not when ξ equals one, but for

$$\xi = \frac{M}{2(N+1)} = \frac{M'}{2(1+1/N)} \quad (26)$$

provided this value is smaller than one.

From equ's. (24) we can extract the amplitude of the field due to the harmonic $n = N + \sqrt{M}$ relative to the amplitude of the fundamental N . For the qualitatively representative case of trapezoidal REC pieces, we obtain from equ. (24a) for that ratio $Q(\nu)$ at $|z| = r$, and for $\xi = 1$

$$Q(\nu) = \left(\frac{r}{r_1}\right)^{\nu \cdot M} \cdot \frac{N-1}{n-1} \cos \frac{\nu M}{2} \cdot \frac{1 - (r_1/r_2)^{n-1}}{1 - (r_1/r_2)^{N-1}} \quad (27)$$

For $r=r_1$, the values for $Q(\nu)$ are uncomfortably large. Fortunately in most applications the largest r/r_1 of concern is, while close to one, still small enough so that the factor $(r/r_1)^{\nu M}$ reduces $Q(\nu)$ to acceptable levels even for the most unfavorable case, $\nu = 1$. Should, however, $Q(1)$ be larger than acceptable, $Q(1)$ can be made to vanish by choosing

$$\xi = 1/(1+N/M) = 1 - 1/(1+M'). \quad (28)$$

For that value of ξ , $Q(\gamma)$ becomes

$$Q(\gamma) = \left(\frac{\gamma}{\gamma_1}\right)^{NM} \cdot \frac{N-1}{n-1} \cdot \cos \xi \pi / M' \cdot \frac{\sin \pi \frac{\gamma-1}{1+M'}}{\sin \frac{\pi}{1+M'}} \cdot \frac{1 - \left(\frac{\gamma_1}{\gamma_2}\right)^{n-1}}{1 - \left(\frac{\gamma_1}{\gamma_2}\right)^{N-1}} \quad (29)$$

For reasonably large values of M , it is unlikely that the worst of these harmonics ($n = N+2M$) will ever cause any problems.

The design represented by equ. (28) means that one has a wedge-shaped non-magnetic space between adjacent pieces of REC. While these gaps could be implemented by having appropriate notches in the magnet assembly fixture, an alternate method of making $Q(1) = 0$ would be the use of a non-magnetic spacer between adjacent REC pieces. For that kind of design it would be advantageous to have spacers of uniform thickness D . Referring to Fig. 5 for the definition of symbols, application of equ. (16a) and (17a) gives for the field in that case

$$\underline{B}^*(z_0) = B_r \sum_{\gamma=0}^{\infty} \left(\frac{z_0}{\gamma_1}\right)^{n-1} \frac{\cos \alpha_0 \cdot \cos \alpha_1}{(n-1)\alpha_0} \times \quad (30a)$$

$$\times \left[\sin(\alpha_0 + \alpha_1(n-1)) - \left(\frac{\gamma_1 \cos \alpha_2}{\gamma_2 \cos \alpha_1}\right)^{n-1} \cdot \sin(\alpha_0 + \alpha_2(n-1)) \right],$$

with

$$D/r_1 = 2 \cos \alpha_0 (\tan \alpha_0 - \tan \alpha_1) \approx 2(\alpha_0 - \alpha_1) / \cos \alpha_0. \quad (30b)$$

$$\tan \alpha_2 = \tan \alpha_0 - \frac{r_1}{r_2} (\tan \alpha_0 - \tan \alpha_1). \quad (30c)$$

To eliminate the harmonic $n = N+M$ in the case where the term proportional to $(r_1/r_2)^{n-1}$ in equ. (30a) can be neglected, one has to satisfy

$$\alpha_1 = (\pi - \alpha_0)/(n-1) = \alpha_0 \frac{M-1}{N+M-1}, \quad (31)$$

giving, with equ. (30b),

$$D/r_1 = \frac{2N}{N+M-1} \cdot \frac{\pi/M}{\cos \pi/M} \quad (32)$$

Formulas for reference pieces with shapes other than trapezoids are easily derived following the same general procedure, but are not given here. From these expressions follows the general rule that the allowed harmonics $n = N + \sqrt{M}$ tend to be the smaller the better the inside REC boundary approximates a circle.

To describe the fields (radially) outside the multipole, we expand B^* in $1/z_0$. By using equ's. (17b) and (18b) instead of equ's. (17a) and (18a), we get instead of equ's. (24):

$$\underline{B}^*(z_0) = \sum_{\sqrt{V}} \underline{b}_{-n} z_0^{-n-1} = \sum_{\sqrt{V}} \left(\frac{r_2}{z_0} \right)^{n+1} \cdot \frac{n}{n+1} \cdot \left(1 - \left(\frac{r_1}{r_2} \right)^{n+1} \right) \cdot \underline{K}_{-n} \quad (32a)$$

$$n = \sqrt{M-N}$$

$$K_{-n} = \cos^{-n}(\epsilon \tilde{\pi}/M) \cdot \frac{\sin \epsilon \tilde{\pi}/M}{n \tilde{\pi}/M} \quad (\text{Trapezoid})$$

$$K_{-n} = \frac{\sin((n-1) \epsilon \tilde{\pi}/M)}{(n-1) \tilde{\pi}/M} \quad (\text{circular arcs}) \quad (32b)$$

Equ. (32a) is valid for $|\underline{z}_0| > r_2/\cos(\xi\pi/M)$ for the trapezoid, and for $|\underline{z}_0| > r_2$ for ^{the} circular arc case. Without going into details, it is clear that at these limits $\underline{B}(\underline{z}_0)$ is somewhat smaller than it is at $|\underline{z}_0| = r_1$. Since $n_{\min} = M-N = N(M'-1)$, the field decays very rapidly with increasing $|\underline{z}_0|$ provided M is reasonably large. Shielding the space radially outside the multipole against these fields will therefore be rarely necessary. We therefore give the expansion for the field perturbation caused by a circular steel shell with $\mu = \infty$ and $|\underline{z}| = R$ without derivation:

$$\Delta \underline{B}_{Steel}^*(\underline{z}_0) = \sum_{\gamma=1}^{\infty} \underline{z}_0^{\gamma-1} (\underline{b}_{-n})^* / R^{2\gamma}$$

$$n = -N + \gamma M \quad (33)$$

\underline{b}_{-n} are the expansion coefficients of the unperturbed field in $1/\underline{z}_0$ as used in equ. (32a). Notice that the fundamental ($n=N$) is not affected by the shield unless M has the exceptionally low value $2N$.

The results of this section show very clearly that the following properties are important for the design of good segmented multipole magnet:

1. The REC should be placed, with the largest possible volume filling factor, as closely to the "business" region as possible, "hugging" the aperture circle as well as possible.
2. In order to produce strong fields of high quality, one should approximate equ. (20) reasonably well, with $M'=8$ easy axis orientations per period being a good guide number.

To arrive at a design, one has to combine these two essential requirements with considerations like availability, or ease of production, of REC pieces of various shapes, ease of assembly, etc. Trapezoidal segments, as discussed above, seem to be a good choice, but it is quite possible that assemblies of tightly packed small rods with circular, hexagonal, or other, cross sections may be preferable under some circumstances.

4.3) The segmented REC quadrupole.

Because of their special importance for accelerators, we discuss some details of quadrupoles, adding to the summaries published elsewhere^{5,6}. Since quadrupoles with trapezoidal segments are quite typical, we restrict the discussion to this specific class of magnets.

From equ. (24a) follows for the fundamental harmonic for $\xi = 1$:

$$\underline{B}^*(z_0) = \frac{z_0}{r_1} \cdot B_r \cdot 2 \cdot \left(1 - \frac{r_1}{r_2}\right) \cdot K_2 \quad (34)$$

$$K_2 = \cos^2(\pi/M) \cdot \frac{\sin 2\pi/M}{2\pi/M}$$

Table 1

M =	4	8	12	16	20	24
K ₂ =	.32	.77	.89	.94	.96	.97

Table 1 shows that in order to get a strong quadrupole, one should choose M=12 or 16. The gradients achievable with a 16-piece quadrupole are impressive, in particular when they are compared with those of conventional quadrupoles. For M=16, $r_2/r_1 = 4$, (which is still quite compact) and $B_r = .95T$ (which is commercially available), one obtains an aperture field of 1.34T. In contrast, a high quality conventional quadrupole is very difficult to make with more than 1T at the aperture, and even that is possible only for fairly large aperture magnets.

High aperture fields are of particular importance for linear accelerators with small apertures. For an aperture with $r_1 = 2\text{mm}$, it is possible to achieve a gradient $B' = 6 \text{ Tcm}^{-1}$, and the diameter of such a quadrupole could be smaller than 2 cm. Clearly, it is impossible to achieve anything resembling this with conventional magnets, and conventional REC quadrupole designs fall short of this gradient by at least a factor of 2.

Fig. 6 shows a schematic cross section of a 16-piece quadrupole, with the easy axis direction indicated in each piece. It follows from that diagram that one needs pieces with five different orientations of the easy axis relative to the trapezoidal shape to make this 16-piece quad. If one rotates all easy axes by 22.5° in the same direction, only four different pieces are required, which may be advantageous for the manufacturer. Since one has, in either case, a reasonably large number of pieces that are supposed to be identical, it may be advantageous to measure magnetization direction and magnitude for each piece, and then assemble the quadrupole in such a way that magnetization errors do the least harm to the field quality. For this reason, it may be a blessing in disguise that with present manufacturing techniques, the individual REC pieces are fairly small. This often forces the use of several layers of REC in the axial direction, increasing the number of pieces and therefore improving the error cancelling statistics.

For a 16-piece quadrupole with $r_1/r_2 = .25$, the first undesirable harmonic ($n=18$) field has, at $|z|=r_1$, an amplitude that is approximately 6% of the fundamental (see equ. (27) for $N=2$). Eliminating that harmonic with a flat sheet of the thickness given by equ. (32), the first non-vanishing harmonic is $n=34$, with a relative amplitude of about 3% at the full aperture. The order of this harmonic is high enough that no attempt has yet been made to eliminate it also.

The fringe fields at the end of a segmented quadrupole (or other multipole) are fairly easily calculated by using the charge sheet model and equ. (11). If the cross sections of the REC pieces are trapezoidal, the charge sheets have rectangular ^{cross sections} and the integrals can be expressed by elementary transcendental functions, making the 3D field calculation rather easy. The relevant formulas are not reproduced here because the fringe fields of REC multipole magnets have some rather remarkable properties (to be discussed in Sect. 4.4) that make fringe field calculations necessary in only very rare instances.

R. F. Holsinger has built a prototype quadrupole with $r_1 = 1.1$ cm; $r_2 = 3$ cm; $M = 16$; and consisting of three 16-piece layers in the axial direction. Comparisons were made between measurements of that magnet, computer runs of that magnet with PANDIRA, and the predictions made with the simple theory presented here. The results obtained with these procedures agreed very well with regard to the amplitude of the quadrupole field and the allowed higher harmonic $n=18$. The only significant, but expected, discrepancy was the presence of the harmonics $n=6, 10, 14$ in the computer model and the real magnet, while these harmonics do not exist in the simple model that assumes $\mu_1 = \mu_2 = 1$. At $|z| = r_1$ the amplitudes of these harmonics were, relative to the quadrupole field, .2% for $n=6$; .1% for $n=14$; and $\ll .1\%$ for $n=10$. While these errors are so small that they are unlikely to cause problems in most applications, one can easily imagine methods to eliminate these harmonics, if necessary. If, for instance, one has a gap between adjacent pieces for the elimination of $n=18$, one could incorporate movable thin strips of soft steel into these gaps to tune away these undesired harmonics. The real magnet also had approximately .5% sextupole, as well as some other multipoles, present. Since the individual REC pieces were not measured, it is expected that these harmonics can be significantly reduced when this is done and

properly taken into account in the assembly. Another obvious tuning method would be the removal or addition of small amounts of REC at appropriate locations, but it is unlikely that such efforts will really be necessary.

4.4) Important practical consequences of applicability of linear superposition principle.

It is obvious that the linear superposition principle is of crucial importance not only for specific important theorems, like the easy axis rotation theorem or the selection rule for possible harmonics (equ. 24a), but to the whole mathematical description of REC magnets presented here. However, there are some very important practical consequences of the linear superposition principle that are obtainable without any mathematical derivations.

We consider first the following combination of two REC multipole magnets: One quadrupole is located, tightly fitting, inside the aperture region of another quadrupole. If each of these quadrupoles alone produces the same gradient, and both quadrupoles are rotated about the common axis by equal amounts in opposite directions, then the gradient in the aperture can be continuously changed between zero and twice the strength of the individual quadrupole. By similarly pairing two dissimilar multipoles, one can make combined function magnets.

Care has to be taken for these combinations of REC magnets, and in particular for combinations of conventional steel magnets with REC magnets, that the REC is not driven into the nonlinear part of the $B_{\eta}(H_{\eta})$ curve. A combination of magnets that would be fairly immune from this danger is a multipole inside the homogeneous field of a coaxial solenoid, since in this case the solenoidal field is everywhere perpendicular to the easy axis.

A different method to modify the effective strength of a REC quadrupole would be to assemble it from quadrupoles of relatively short axial lengths whose quadrupole field orientations can be adjusted. While this would be fairly easy to do, such a scheme obviously modifies the optical properties of the system in a non-trivial way, and this aspect of such a system is currently under investigation(8).

Another important application of the superposition principle is the treatment of the fringe fields at the ends of multipole magnets. We deal here with two distinctly different aspects of fringe fields that are both very simple and important.

First we consider a multipole of finite physical length L whose left end is cut off in an arbitrary fashion, and whose right end is shaped such that the left end would fit it perfectly, without forming any gap. (See Fig. 7) Another way to express that geometry is to state that the length of REC along any line parallel to the axis is either L or zero. Keeping the left end of the multipole fixed in space, we first consider the field quantity $G_1(r, \varphi, z)$ produced by a semi-infinite multipole, with $G_0(r, \varphi)$ representing the 2D field deep inside where it does not depend on z . Then the field quantity $G(r, \varphi, z)$ produced by a multipole of length L is given by

$$G(r, \varphi, z) = G_1(r, \varphi, z) - G_1(r, \varphi, z-L). \quad (35)$$

If we now calculate the optically important $\int_{-\infty}^{\infty} G(z) dz$, it is easy to see that equ. (35) leads to

$$\int G(r, \varphi, z) dz = L \cdot G_0(r, \varphi). \quad (36)$$

This equation says not only that the effective length for the fundamental harmonic of interest equals the physical length of the multipole, but also that the integral over a field quantity vanishes if that field quantity is zero in the 2D cross section!

Next, we consider the properties of the fringe fields produced by a semi-infinite multipole, produced by cutting an infinite multipole by the x-y plane at $z=0$ (see Fig. 8), i.e., we look at the fringe field function $G_1(z)$ for the specific case of the "square" end. If $V_1(r, \varphi, z)$ is the scalar potential produced by the multipole located at $z > 0$, then the scalar potential produced by the multipole located at $z < 0$ must be $V_1(r, \varphi, -z)$. If $V_1(r, \varphi, z)$ is the scalar potential inside the infinitely long multipole, the following obviously must hold:

$$V_1(r, \varphi, z) + V_1(r, \varphi, -z) = V_0(r, \varphi). \quad (37)$$

Applying to this equation the appropriate operator to get the field quantity $G_1(r, \varphi, z)$ of interest, we get, if no derivative with respect to z is involved:

$$G_1(r, \varphi, z) + G_1(r, \varphi, -z) = G_0(r, \varphi) = 2 G_1(r, \varphi, 0) \quad (38)$$

From this follows that

$$\int_{-\infty}^{z_1} G_1(r, \varphi, z) dz = z_1 \cdot G_0(r, \varphi) \quad (39)$$

if z_1 is sufficiently large. This means that the effective boundary is at $z=0$, and that the fringe field integral over a field quantity vanishes if that quantity is zero in the 2D cross section. Notice that this

statement is stronger than the one made above with respect to equ. (36), which required integration over the fringe fields of both ends.

If the operator to obtain the field quantity of interest is proportional to $(\partial/\partial z)^m$, we get instead of equ. (38)

$$G_1(r, \varphi, z) = -(-1)^m G_1(r, \varphi, -z). \quad (40)$$

Integrating this $G_1(r, \varphi, z)$ over the fringe field region gives zero when $m \geq 2$, but not necessarily when $m = 1$.

Appendix

Using equ. (14) in equ. (13), one of the two integrals that have to be evaluated in equ. (13) is

$$I_1 = \frac{1}{2\pi i} \int \frac{\partial H_{cy}/\partial x}{z_0 - x - iy} dx dy$$

Carrying out the integration over x first, and integrating by parts, one obtains

$$I_1 = \frac{1}{2\pi i} \oint \frac{H_{cy}}{z_0 - z} dy - \frac{1}{2\pi i} \int \frac{H_{cy}}{(z_0 - z)^2} dx dy.$$

Included in the integration area is a thin strip of vacuum outside the REC. $H_{cy} = 0$ there, so that the line integral over y vanishes. Applying the same technique to the other integral necessary for the evaluation of the integral in equ. (13), one obtains equ. (15).

ACKNOWLEDGMENTS

I would like to thank J. A. Farrell, T. D. Hayward, E. A. Knapp (Los Alamos Scientific Laboratory), and R. L. Gluckstern (University of Maryland) for their active interest, support and discussions of this work.

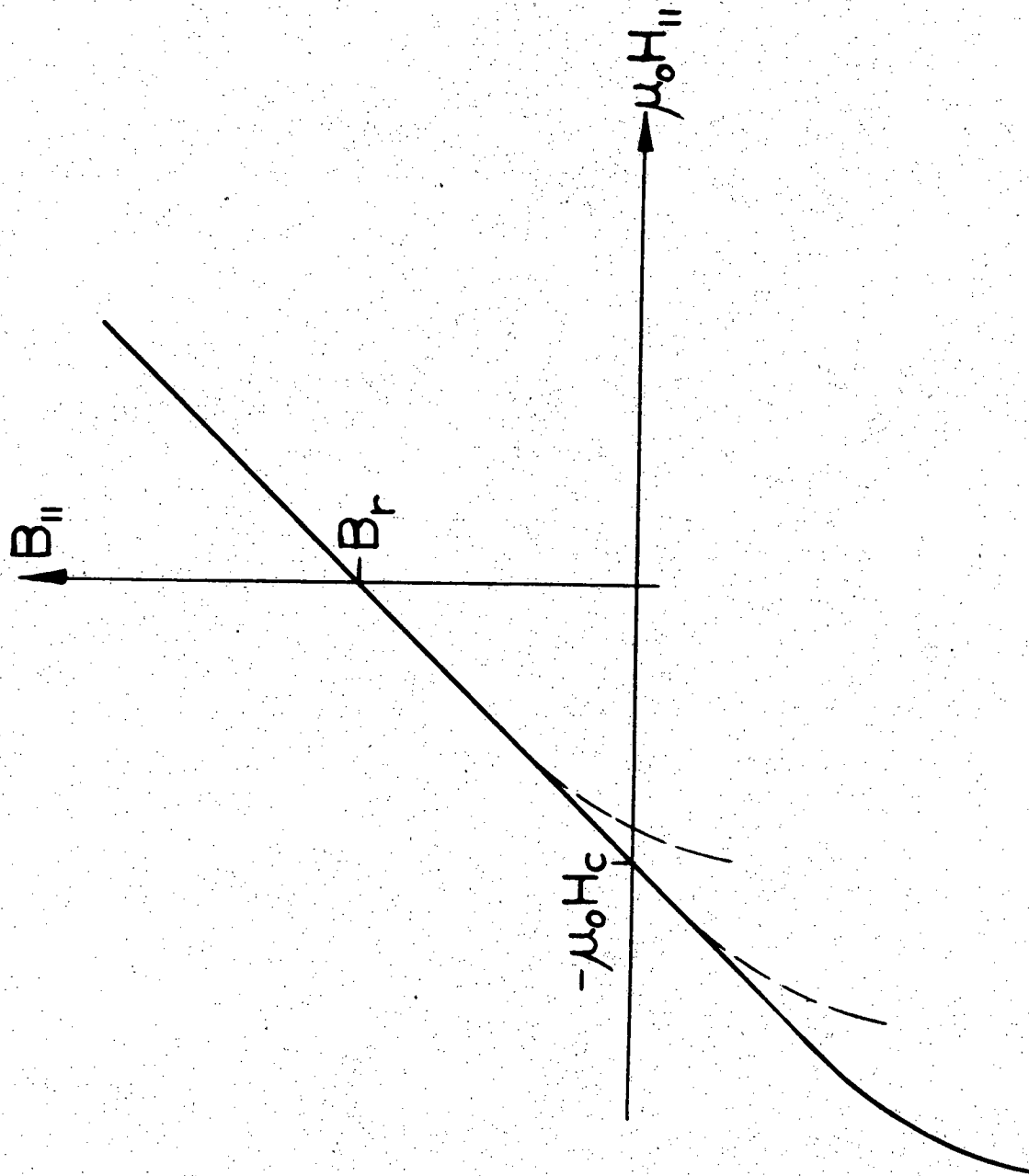
M. Kaviany (Lawrence Berkeley Laboratory) made some useful computer runs and R. Holsinger shared the results of his computer runs and practical experiences and contributed greatly with several useful suggestions and many stimulating discussions.

REFERENCES

1. K. J. Strnat, G. I. Hoffer: Techn. Report, AFML-TR-65-446, Wright Paterson Air Force Base, (1966); see also J. B. Y. Tsui, D. J. Iden, K. J. Strnat, A. J. Evers; IEEE Transactions on Magnetics No. 2, p 188, (1972).
2. M. McCaig: Permanent Magnets in Theory and Practice; J. Wiley & Sons, (1977).
3. K. Halbach: Nucl. Instr. Meth. 78, p 185 (1970).
4. J. P. Blewett: BNL Internal Report, AADD-89, (1965).
5. K. Halbach: Proc. 1979 Particle Accelerator Conference; IEEE Transactions on Nuclear Science; Vol. NS-26; p 3882, (1979).
6. R. F. Holsinger, K. Halbach: Proc. 4 Intern. Workshop on Rare Earth Cobalt Permanent Magnets, p 37, (1979).
7. Description to be published by R. F. Holsinger, K. Halbach.
8. R. L. Gluckstern, private communication.

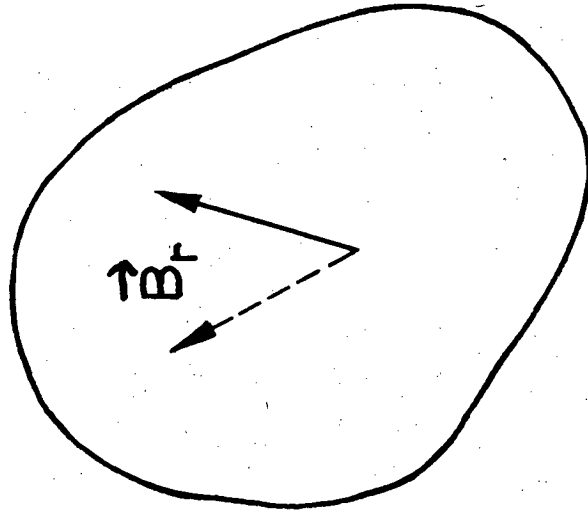
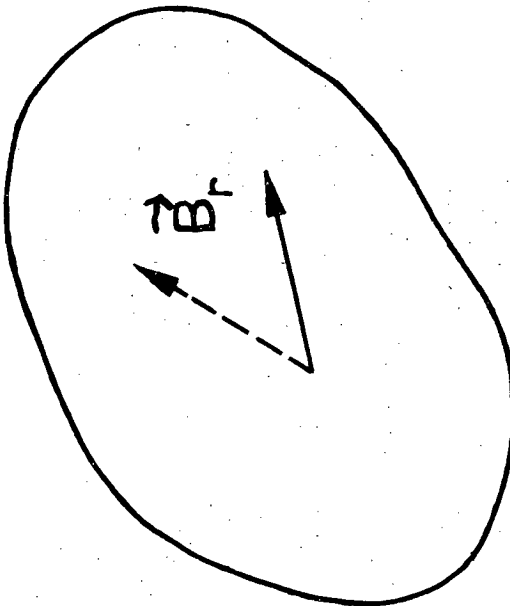
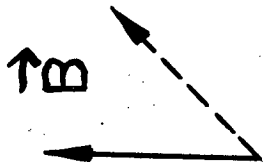
FIGURE CAPTIONS

1. $B(H)$ - curve in direction parallel to easy axis.
2. Effect of rotation of easy axes on magnetic field.
3. Integration path for calculation of field inside the REC material.
4. One piece of a segmented REC multipole.
5. One piece of a segmented REC multipole with flat sheet spacer.
6. Schematic cross section of a 16 piece REC quadrupole.
7. Geometry of specific finite length REC multipole.
8. Fields at the end of a REC multipole.



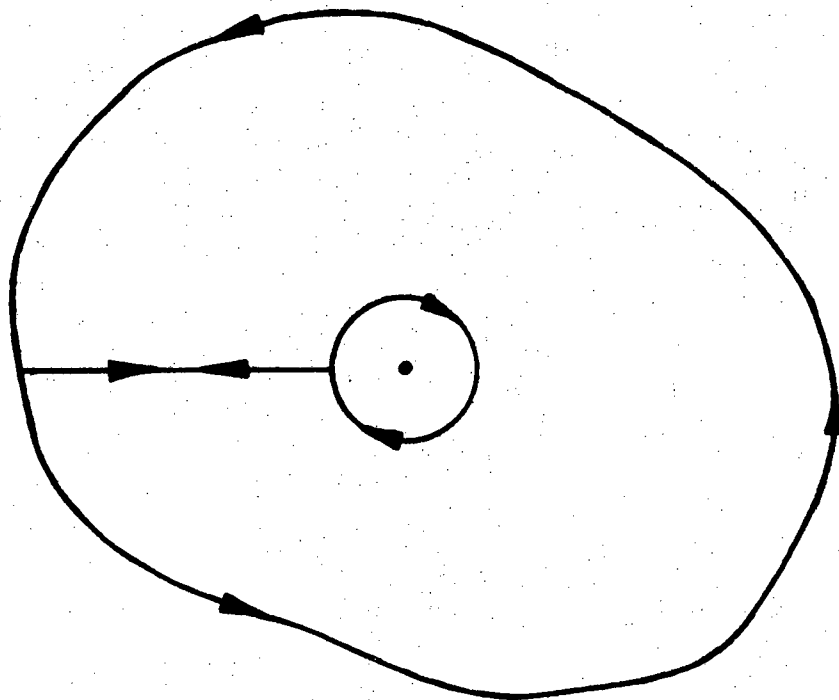
XBL 797-10554

Figure 1



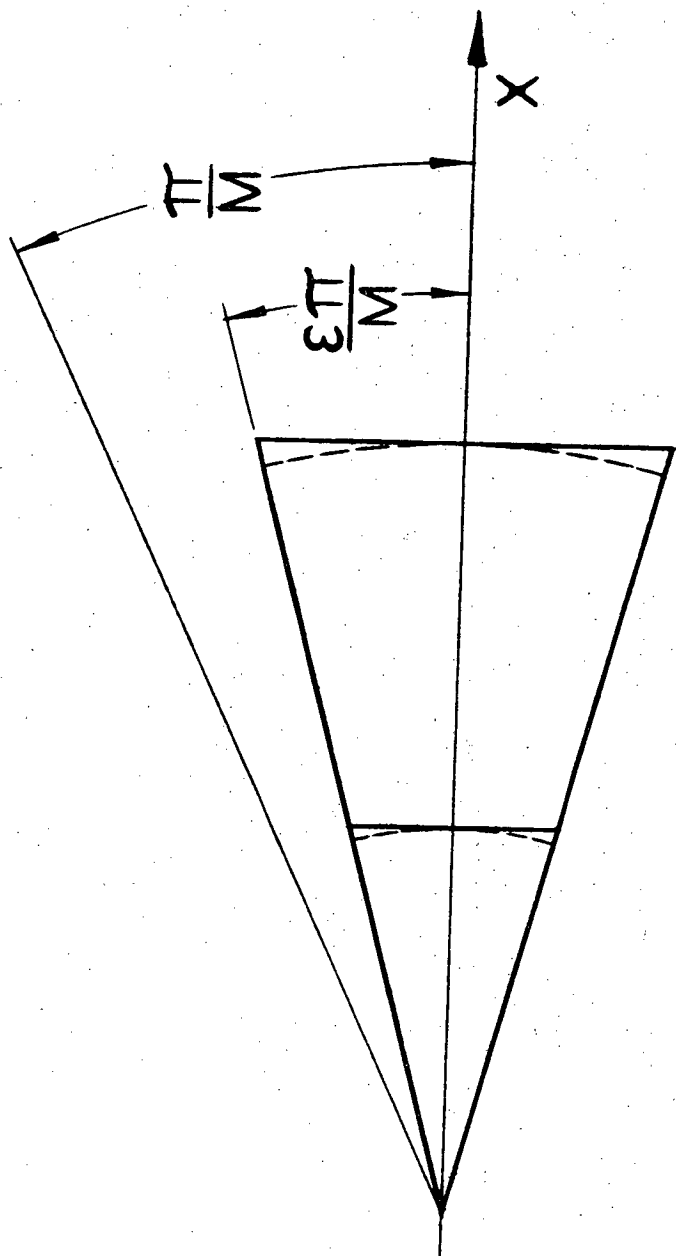
XBL 797-10558

Figure 2



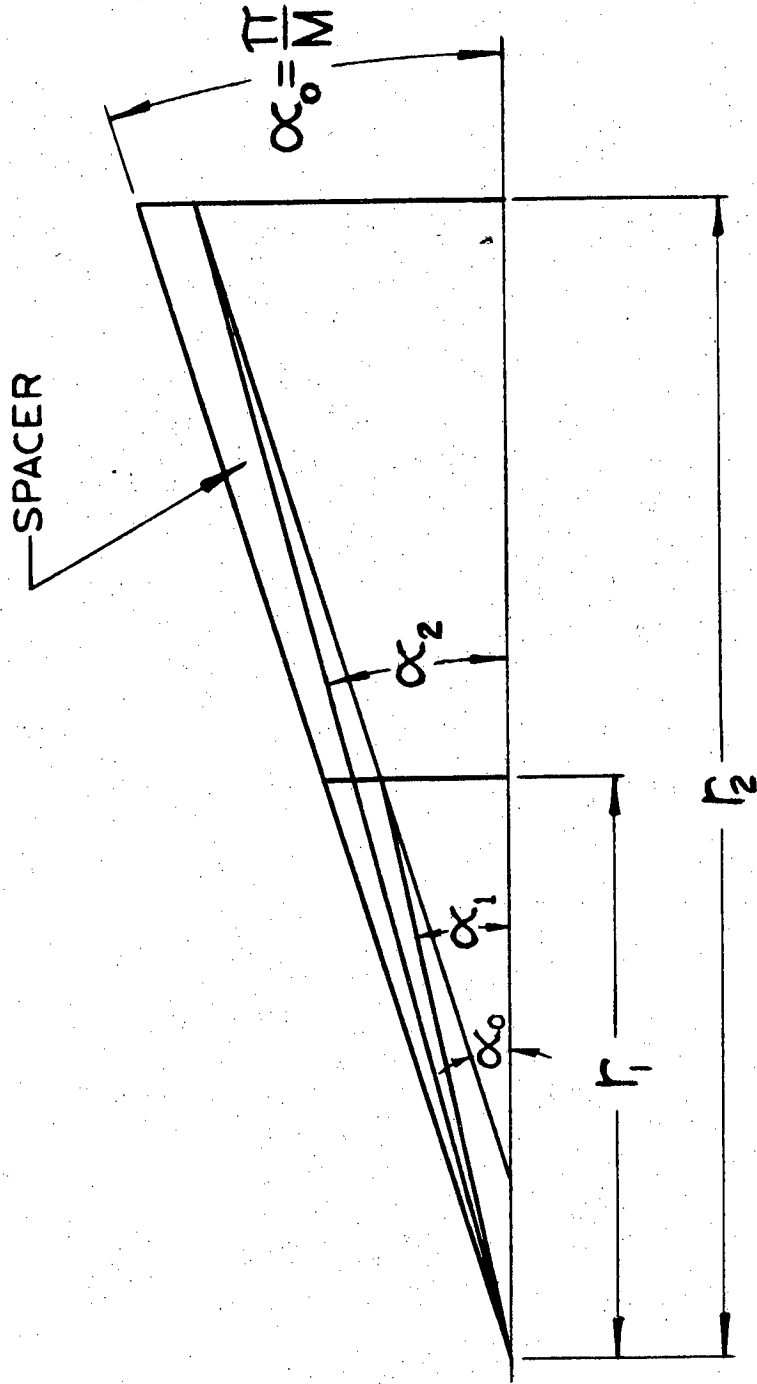
XBL 797-10559

Figure 3



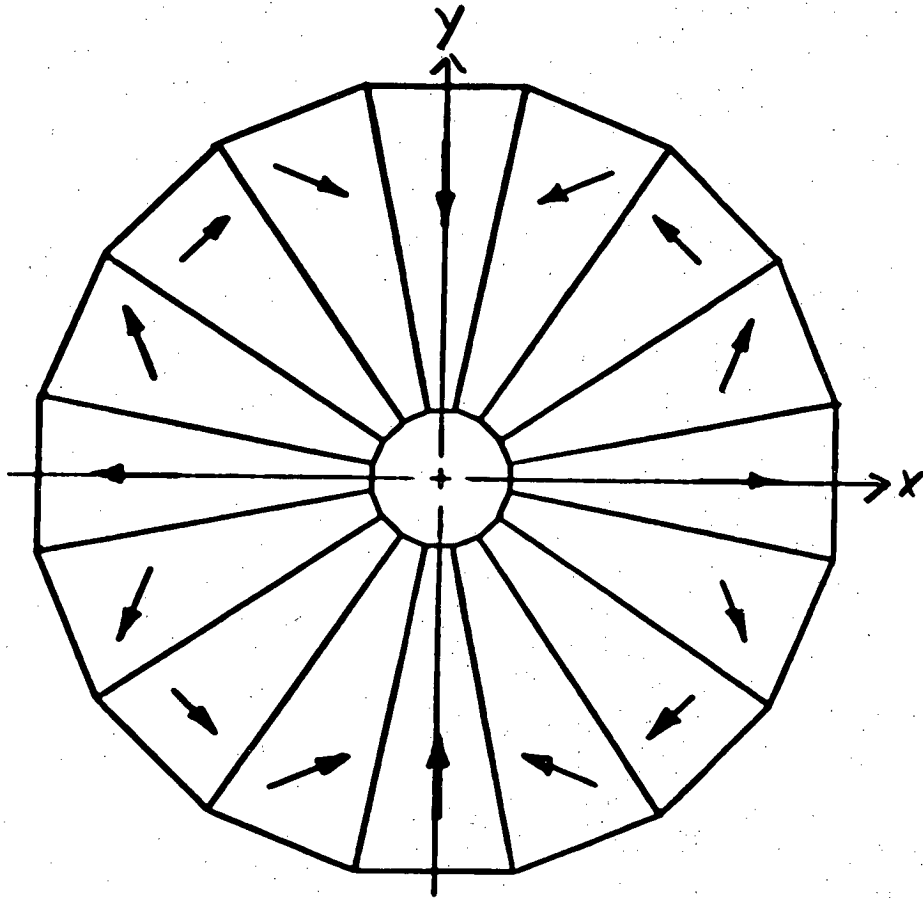
XBL 797-10555

Figure 4



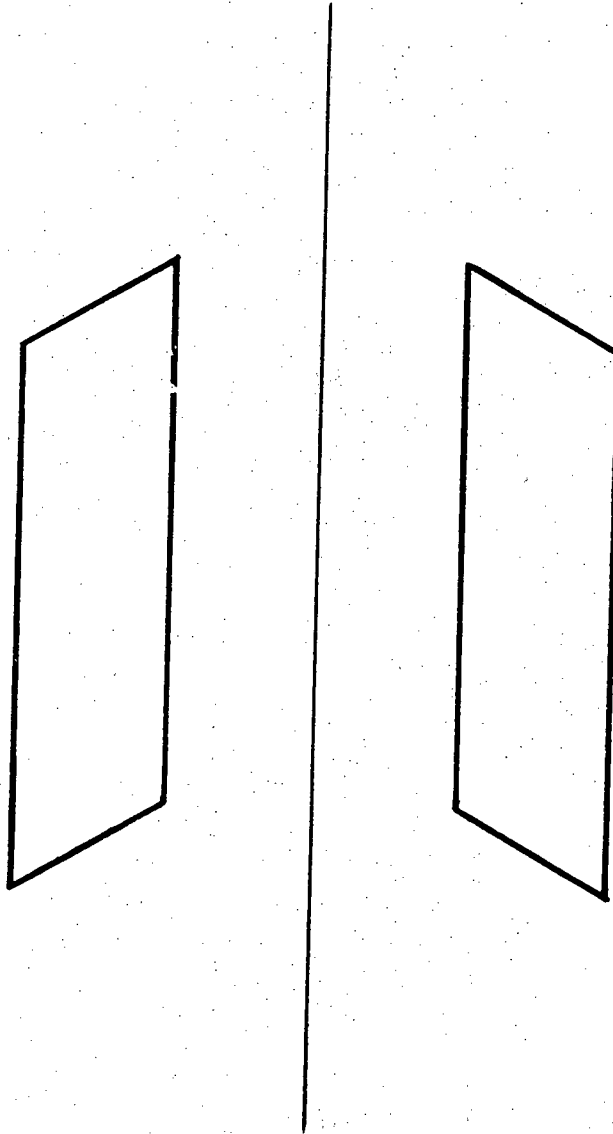
XBL 797-10546

Figure 5



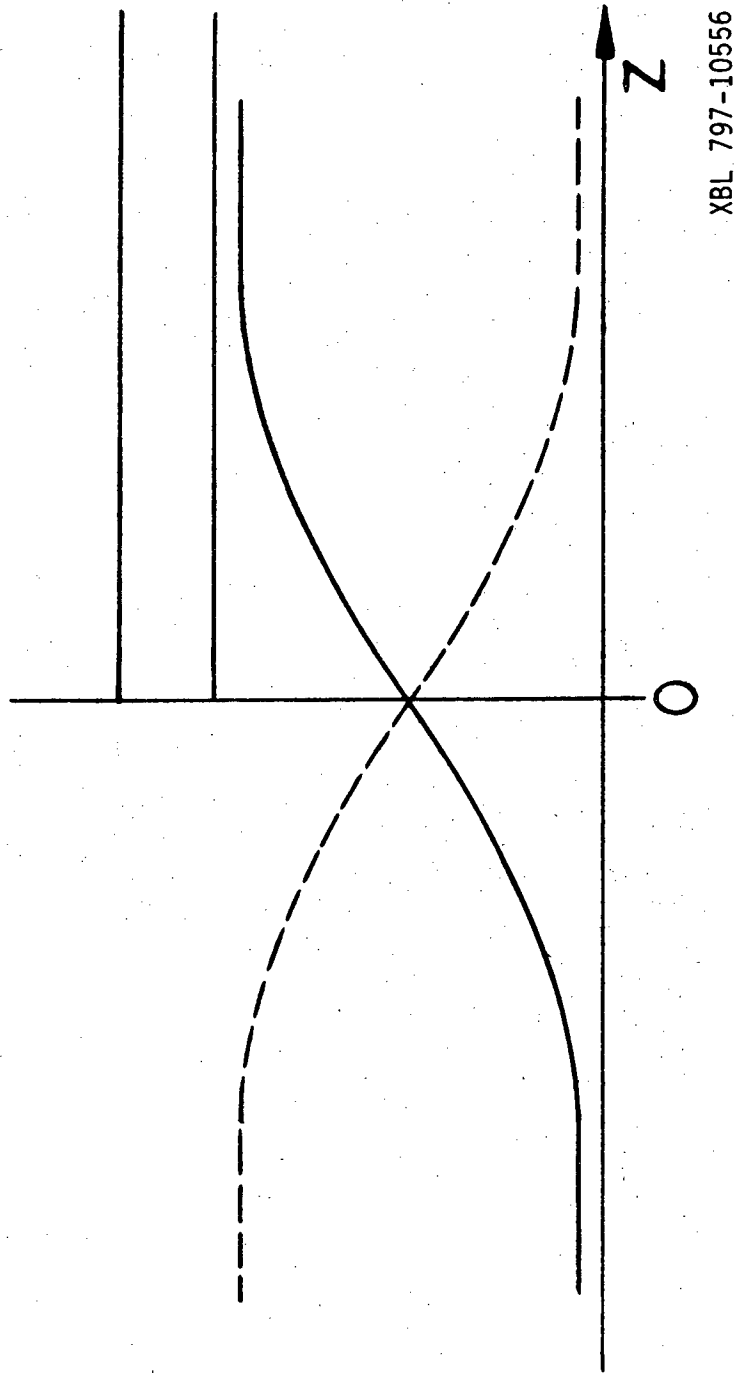
XBL 792-8538

Figure 6



XBL 797-10557

Figure 7



XBL 797-10556

Figure 8

This report was done with support from the Department of Energy. Any conclusions or opinions expressed in this report represent solely those of the author(s) and not necessarily those of The Regents of the University of California, the Lawrence Berkeley Laboratory or the Department of Energy.

Reference to a company or product name does not imply approval or recommendation of the product by the University of California or the U.S. Department of Energy to the exclusion of others that may be suitable.

TECHNICAL INFORMATION DEPARTMENT
LAWRENCE BERKELEY LABORATORY
UNIVERSITY OF CALIFORNIA
BERKELEY, CALIFORNIA 94720